Proceedings of the ASME 2013 Pressure Vessels & Piping Division Conference
PVP2013
July 14-18, 2013, Paris, France

PVP2013-97534

ACOUSTIC RESONANCE EXPERIMENTS IN A RESERVOIR - PIPELINE - ORIFICE SYSTEM

Arris S. TIJSSELING
Department of Mathematics and Computer Science
Eindhoven University of Technology
P.O. Box 513, 5600 MB Eindhoven
The Netherlands
E-mail: a.s.tijsseling@tue.nl

Qingzhi HOU
School of Computer Science and Technology
Tianjin University
Tianjin
China
E-mail: darcy.hou@gmail.com

Bjørnar SVINGEN
Rainpower Norge AS
S.P. Andersens veg 7
N-7465 Trondheim
Norway
E-mail: bjoernar.svingen@rainpower.no

Anton BERGANT
Litostroj Power d.o.o.
Litostrojska 50
1000 Ljubljana
Slovenia
E-mail: anton.bergant@litostrojpower.eu

ABSTRACT

Acoustic resonance in liquid-filled pipe systems is an undesirable phenomenon that cannot always be prevented. It causes noise, vibration, fatigue, instability, and it may lead to damage of hydraulic machinery and pipe supports. If possible, resonance should be anticipated in the design process and be part of the hydraulic-transients analysis.

This paper describes acoustic resonance tests carried out at Deltares, Delft, The Netherlands, within the framework of the European Hydralab III programme. The test system is a 49 m long pipeline of 206 mm diameter that is discharging water from a 24 m high reservoir through a 240 mm^2 orifice to the open atmosphere. The outflow is partly interrupted by a rotating disc which generates flow disturbances at a fixed frequency in the range 1.5 Hz to 100 Hz. In previous studies [1, 2] a similar system was analysed theoretically. Herein experimental data are presented and interpreted. Steady oscillatory behaviour is inferred from pressures measured at four different positions along the pipeline. Heavy pipe vibration during resonance was observed (visually and audibly) and recorded by a displacement transducer.

Key words
Water hammer; Hydraulic transients; Acoustic resonance; Impedance; Orifice; Rotating valve; Experiment.

BACKGROUND

This work is part of the scientific programme *"Unsteady friction in pipes and ducts"* [3] which refers to the one-dimensional (1D) mathematical modelling of skin friction in unsteady pipe flow. In (quasi-)steady 1D models skin friction is a function of flow rate only, but in many unsteady friction models it is a function of both flow rate and flow acceleration (or pressure gradient). To validate the prevailing unsteady friction models for turbulent pipe flow, the present project aims at measuring the features that characterise unsteady friction in a large-scale pipeline, where the large scale implies large Reynolds numbers. The pipeline has a diameter of 0.2 m, a length of about 50 m and is supplied with water from a 25 m head reservoir at its upstream end. The measurements were divided into three groups and set-ups. Group A experimented with non-reversing, accelerating and decelerating flows with a free surface at the downstream end of the pipeline. Group B experimented with reversing, accelerating and decelerating flows with a pressurised air tank at the downstream end (with tank pressures of 7-8 bar). Groups A and B measured in flows with (quasi-)steady Reynolds numbers (Re) between 50000 and 400000 involving mass accelerations with flow fields that are uniform in the axial direction [4-6]. In contrast, Group C tested with acoustically oscillating flow fields that are not uniform in the axial direction. The key element was a rotating valve [7]

that generated harmonically oscillating flow rates and pressures. The flow accelerations are then linearly proportional to the frequency of oscillation.

The results of group C are presented and analysed herein with an emphasis on the resonance behaviour of the system. The theoretical considerations in the previous studies [1, 2] are employed in the interpretation of the measurements.

LABORATORY SET-UP

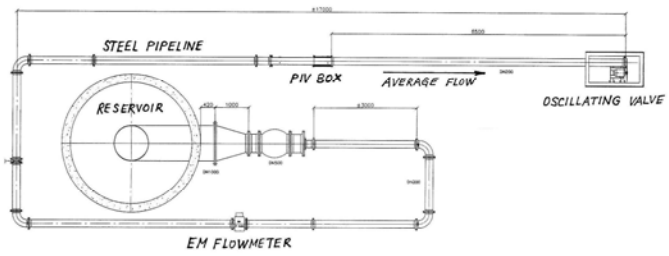

Figure 1 Sketch of reservoir - pipeline - orifice system.

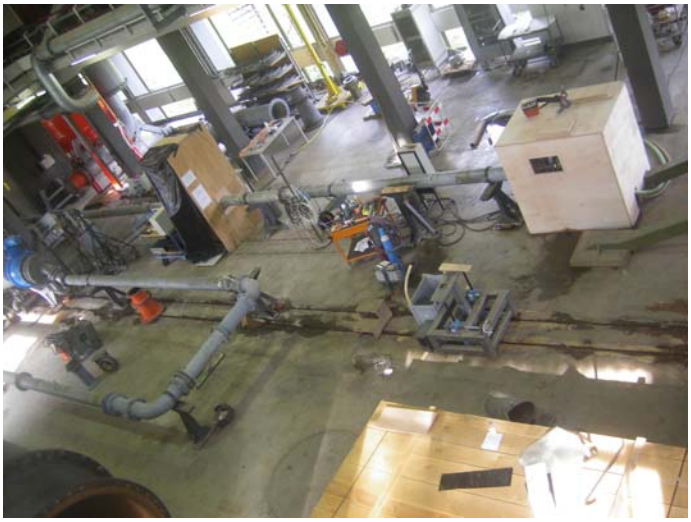

Figure 2 Photo of reservoir - pipeline - orifice system.

Test rig

The stainless steel pipeline has a total length of about 50 m, an inner diameter of 206 mm and a wall thickness of 5.9 mm (Figs 1, 2). The pipeline is connected to a water tower via a ball valve of 500 mm diameter, a 1 m long tapered section and a 25 m long (mostly) vertical pipe of 1000 mm diameter leading to a free surface at an elevation of 23.75 above the central axis of the ball valve. At the downstream side of the ball valve the pipeline curves downwards to a 335 mm lower level (Fig. 3). This curved section contains a rubber bellows (compensator) which could not be removed from the apparatus. Instead it was "fixed" against radial expansion by a tightening belt. The DN200 pipe at the upstream end of the bellows is fixed axially to the DN500 pipe; downstream there are 12 pipe supports restraining pipe movement. The length of the pipeline is 51.55 m from the downstream orifice (rotating valve) up to the water tower's 1000 mm pipe and 48.95 m from the rotating valve up to the downstream side of the 500 mm ball valve (both including curved section). The downstream termination of the pipeline has a 1-inch valve, a 2-inch valve, and a 100 mm × 8 mm aperture that can be (partly) covered by a solid latch (to regulate the average flow velocity) and a rotating disc (to induce a steady oscillation). The rotating disc has a diameter of 526 mm and three sinusoidal periods with amplitude 10 mm as displayed in Figs 4-7. The outflow area varied between 80 and 240 mm^2 for controlled frequencies of rotation between 1.5 Hz and 100 Hz.

The main differences with the pipeline used by Groups A and B [4-6] are: a different downstream termination, a longer pipeline upstream of the PIV box, no flow straightener 19 m upstream of the rotating valve, no rubber bellows (compensator) downstream of the ball valve and a different connection to the reservoir (water tower).

Figure 3 Photo of upstream connection with ball valve.

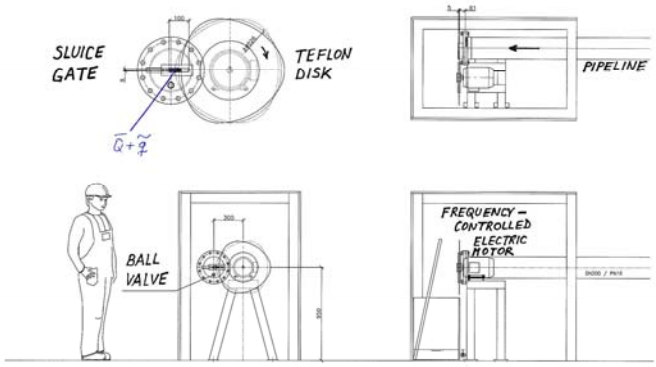

Figure 4 Sketch of rotating-valve system.

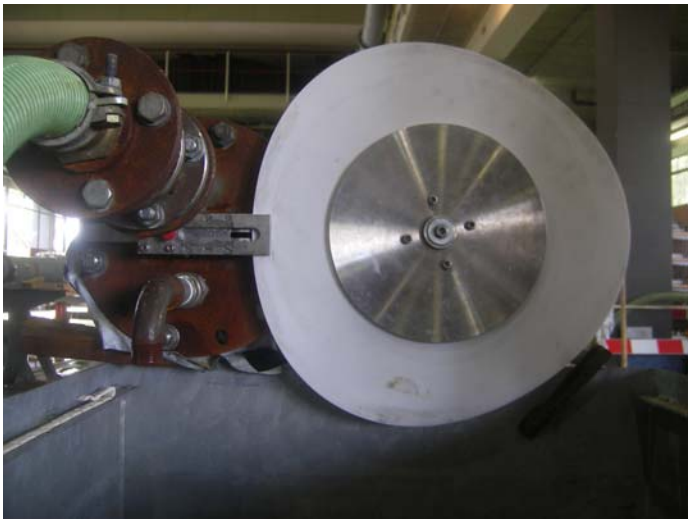

Figure 5 Photo of rotating disc.

Figure 6 Photos of orifice (left) and rotating disc (right).

Figure 7 Photos of downstream end (left) and frequency converter (right).

Instrumentation

The system was equipped with: *static pressure transducer* (PDCR-4010, static pressure gauge, maximum pressure 5 bar absolute; the static pressure transducer is located at the ball valve); *dynamic pressure transducers* (Kulite model HKM-150-375M-50Bar-A, piezoelectric pressure transducer, maximum pressure 50 bar absolute; the dynamic pressure transducers are located 0.42 m (K1), 6.84 m ($K2^a$), 17.04 m ($K2^b$), 31.71 m (K4) and 46.84 m (K3) upstream of the rotating valve (excluding flange thickness of 0.02 m at downstream end)); *differential pressure gauge* (Rosemount 3051CD, differential pressure gauge, maximum pressure difference 7.5 mbar, response time 700 ms, 0.1% accuracy; the differential pressure gauge is connected to selected pressure taps); *flow meter* (ABB electromagnetic flow meter, fast response, 0.35% error at 19.5 litres/s, 5% inaccuracy at velocities below 0.5 m/s, not fast enough for waterhammer tests; all performed tests have been for velocities below 0.5 m/s, which corresponds to a flow rate of 16.5 litres/s, and therefore the measured flow rates will have an inaccuracy of the order of 10%; the flow meter is located 19.83 m downstream of the ball valve. *Note:* Low steady flow rates have been measured by the volumetric method, that is: measuring by hand the time needed to collect a certain amount of discharged water.); *displacement transducer* (ILD1401-250mm, laser-Doppler displacement transducer, maximum displacement 250 mm; the displacement transducer is located 5.24 m upstream of the rotating valve (excluding flange thickness of 0.02 m at downstream end) and measures axial displacements, see Fig. 8); *thermometers* (Rosemount model E32100, resistance thermometer; this thermometer is located in the reservoir tower. A second thermometer is located 2 m downstream of the flow meter.); *hot film sensors* (Dantec Dynamics. The wall shear stress is measured at three circumferential positions at two different axial locations along the pipeline. One set of three hot film sensors is located at the PIV box and another set is located 1.15 m upstream of the PIV box.); *PIV equipment* (The PIV box is located 7.59 m upstream of the rotating valve (excluding flange thickness of 0.02 m at downstream end)). The *frequency converter* sets a fixed rpm of the rotating disc in the range 1.5 Hz to 100 Hz. The disc stops rotating below 1.5 Hz, because that is the limit for stable motor torque needed from the converter/motor system.

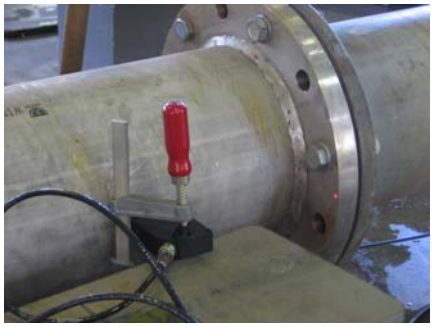

Figure 8 Laser-Doppler displacement transducer.

Data acquisition

Two computers with in-house (Deltares) software were used for collecting the data. One computer captured the huge amounts of data comprising the PIV images; the other captured all remaining signals at a sampling rate of 1000 Hz in the unsteady flow tests.

TEST PROGRAMME

The following tests have been performed: *steady and quasi-steady flow* (to estimate skin friction factor and orifice resistance, to calibrate the hot-film sensors; water leaves the system through the orifice and/or valves in the steady tests and with a slowly rotating disc in the quasi-steady tests; Re = 1000 to 150000); *waterhammer* (to estimate wavespeed and damping rate; manual closure of the downstream 1-inch valve; $\mathrm{Re}_{\mathrm{initial}}$ = 25000); *steady oscillatory flow* (to estimate resonance frequencies and wall shear stresses; water leaves the system via the rotating valve; $\mathrm{Re}_{\mathrm{average}}$ = 22000). Nearly two hundred experimental runs have been recorded.

Filling

The eight pumps feeding the water tower were switched on with the ball valve shut and its bypass open. In this way the pipeline was filled with the 2-inch valve (primarily used for flushing) at the downstream end fully open. Then the ball valve was opened and its bypass valve closed. To de-air the system, the water was running for about half an hour with all (de-aeration) taps open, until audible and visible air escape had stopped.

Testing

All taps were closed, including those of the differential pressure gauge in the unsteady tests. The measuring equipment was switched on and 10 minutes was waited for warming up of the hot films. The valve rotation frequency ranged from 1.5 Hz to 50 Hz in steps of 1 Hz and from 50 Hz to 100 Hz in steps of 10 Hz. Around (audible) resonance frequencies the steps were reduced to 0.25 Hz. After each applied frequency step the recording was stopped (for a few minutes) until the signals on the screen stabilised to a steady oscillatory state.

EXPERIMENTAL RESULTS

Orifice resistance and skin friction factor

The resistance factor of the orifice is estimated by $\xi := \dfrac{2P}{\rho V^2}$ from gauge pressure $P = P(\mathrm{K1})$ and steady flow velocity V. The mass density of water is denoted by ρ. The Darcy-Weisbach friction factor is estimated by $\lambda := \dfrac{2D}{\Delta L}\dfrac{\Delta P}{\rho V^2}$ from ΔP [here $P(\mathrm{K2}) - P(\mathrm{K1})$] and V. The inner diameter of the pipe is D and ΔL is the distance between the pressure transducers located at the positions K1 and K2 (Fig. 9). If ΔP is not accurate because ΔL is too small (ΔP is a small difference between two large numbers), then λ can be estimated from two different pressure measurements at the same location. Here P_1, V_1 and P_2, V_2 are pressure (measured at position K1 at distance L_1 from the reservoir) and velocity in different steady states 1 and 2, respectively, P_0 is the constant reservoir pressure, λ_1 and λ_2 are the unknown friction factors, and $\varepsilon = \lambda_2 - \lambda_1$ is assumed to be small. Keep in mind that ε depends on Re. With

$$P_1(\mathrm{K1}) = P_0 - \lambda_1 \frac{L_1}{D}\frac{\rho V_1^2}{2} \quad \text{and} \quad P_2(\mathrm{K1}) = P_0 - \lambda_2 \frac{L_1}{D}\frac{\rho V_2^2}{2}$$

it follows that (elimination of P_0)

$$\lambda_1 = \frac{2D}{L_1\rho}\frac{P_2(\mathrm{K1}) - P_1(\mathrm{K1})}{V_1^2 - V_2^2} + \varepsilon\frac{V_2^2}{V_1^2 - V_2^2} \quad \text{or}$$

$$\lambda_2 = \frac{2D}{L_1\rho}\frac{P_2(\mathrm{K1}) - P_1(\mathrm{K1})}{V_1^2 - V_2^2} + \varepsilon\frac{V_1^2}{V_1^2 - V_2^2}.$$

Neglecting the last terms gives the same estimate ($\lambda_1 = \lambda_2$) of the friction factor λ. This one-point procedure yields an average friction factor for Reynolds numbers between Re_1 and Re_2; it implicitly includes minor losses at the bends. *Note:* Taking $V_2 = 0$ gives $P_2 = P_0$ and $\lambda = \lambda_1 = \dfrac{2D}{L_1\rho}\dfrac{P_0 - P_1}{V_1^2}$ which is the conventional two-point formula based on ΔP with K2 located at the reservoir.

The values for λ estimated from the measurements by the one-point method are in the range 0.018–0.044. This compares to values $\lambda = 0.02$ based on the Moody diagram.

The measured values for ξ are in the range 1800–7600 for a fully open to a partly closed orifice. This compares to the semi-empirical resistance coefficient $\xi = 4821$ obtained from

$$\xi := \left(\frac{A}{C_d\, A_{\mathrm{or}}}\right)^2,$$

where A = 33329 mm^2 is the cross-sectional area of the pipe, A_{or} = 800 mm^2 is the maximum area of the orifice and C_d = 0.6 is the assumed coefficient of discharge.

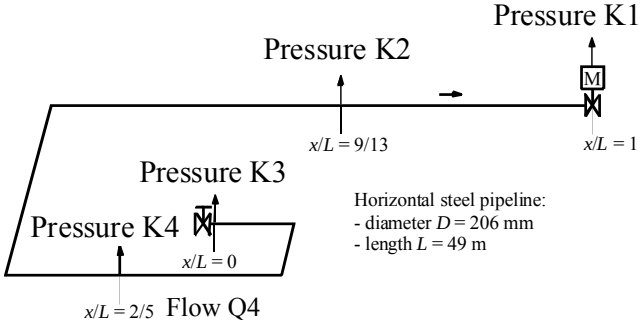

Figure 9 Positions K1–K4 of dynamic pressure transducers and position Q4 of flow meter.

Wavespeed and phase velocity

The theoretical wavespeed for the pipeline is c = 1263 m/s based on the Korteweg formula

$$c := \sqrt{\frac{K^*}{\rho}} \quad \text{with} \quad \frac{1}{K^*} := \frac{1}{K} + \frac{D}{Ee} ,$$

where D = inner pipe diameter, E = Young modulus of pipe material, e = wall thickness, K = bulk modulus of liquid and K^* = effective bulk modulus including pipe wall elasticity.

The pressure wavespeed or phase velocity is estimated from:

i) measured ΔP (Joukowsky pressure rise), $c = \dfrac{\Delta P}{\rho \Delta V}$,

ii) measured Δt (wave-front travel-time), $c = \dfrac{\Delta L}{\Delta t}$,

iii) measured f_0 (frequency of free vibration), $c = 4L\, f_0$.

Note: The methods *i)* and *ii)* give a direct estimate of the wavespeed. Method *iii)* gives the phase velocity which depends on the end conditions (and the wave reflections there). Wavespeed and phase velocity are not the same in dispersive systems.

Using method *i)* and ignoring two outliers in ten waterhammer tests, all estimated wavespeeds were in between 1000 and 1100 m/s. Method *ii)* appeared to be quite inaccurate, because it was difficult to identify the precise position of the wavefront. Using method *iii)* and ignoring two outliers in ten waterhammer tests, all estimated wavespeeds were in between 1000 and 1025 m/s.

Pressures

Steady oscillatory pressures for excitation frequencies of 5, 10 and 12.5 Hz are shown in Fig. 10. These are smooth sinusoidal signals of almost constant amplitude, although a small beat is observed most prominently in the 10 Hz signal.

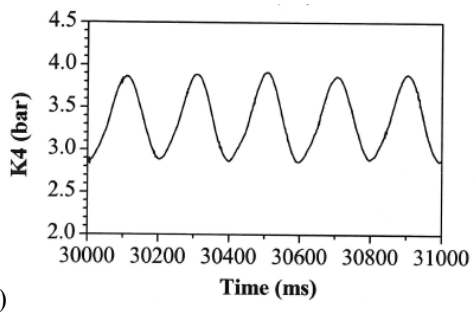

(a)

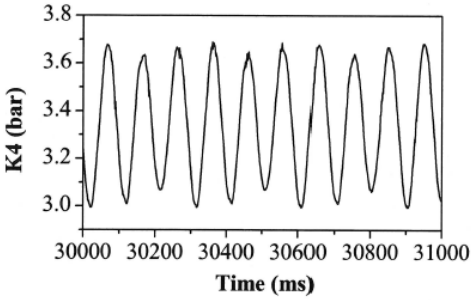

(b)

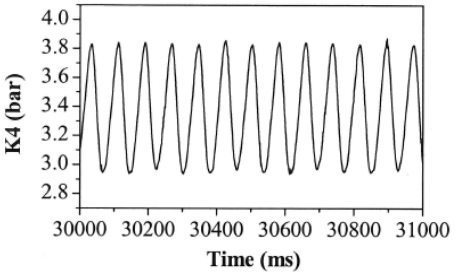

(c)

Figure 10 Pressures (absolute) measured at position K4 for three exciting frequencies: (a) 5 Hz, (b) 10 Hz and (c) 12.5 Hz.

Flow rates

Steady oscillatory flow rates for excitation frequencies of 5, 10 and 12.5 Hz are shown in Fig. 11. These signals are not smooth, because the electromagnetic flow meter is not able to accurately measure unsteady flows. However, the signals give the average flow rate and they give a rough indication of the flow-rate amplitude.

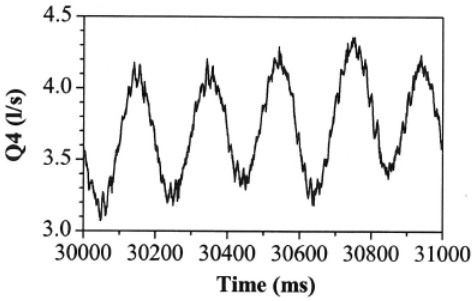

(a)

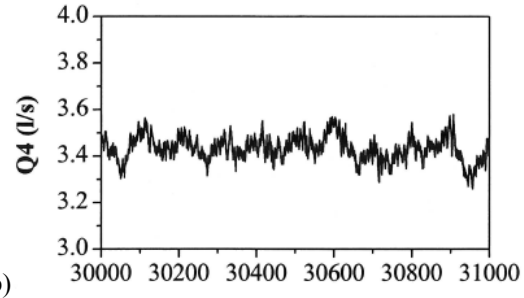

(b)

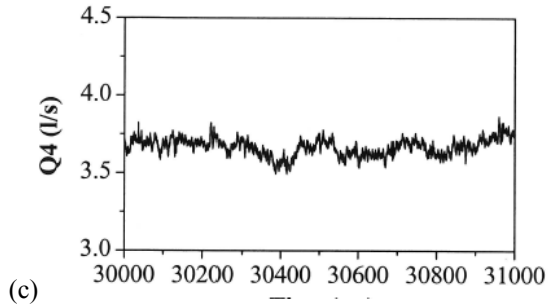

Figure 11 Flow rates measured for three exciting frequencies: (a) 5 Hz, (b) 10 Hz and (c) 12.5 Hz.

Displacements

Axial pipe displacements observed for excitation frequencies of 5, 10 and 12.5 Hz are shown in Fig. 12. The largest values at 12.5 Hz indicate visible and audible resonance, where the whole system was shaking.

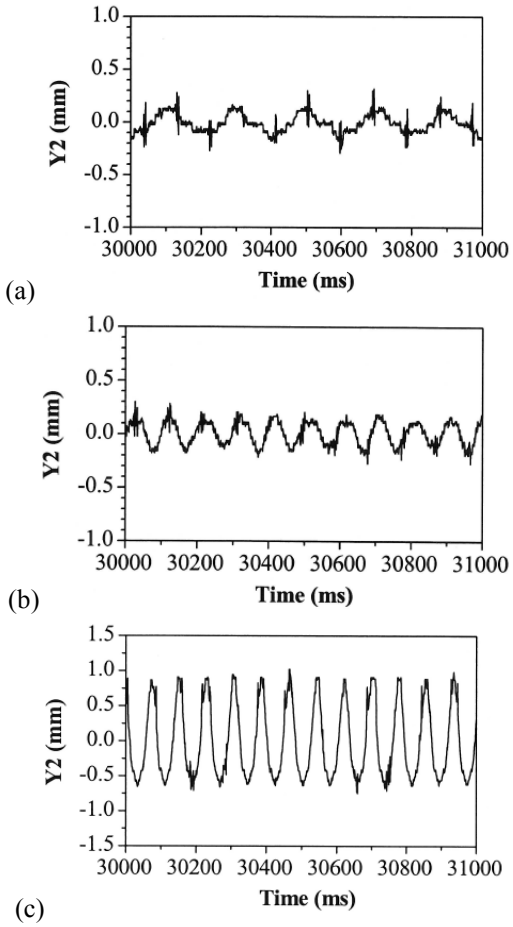

Figure 12 Axial displacements measured for three exciting frequencies: (a) 5 Hz, (b) 10 Hz and (c) 12.5 Hz.

Pressure amplitude versus excitation frequency

The pressure-amplitude versus excitation-frequency diagram (Fig. 13) shows the resonance behaviour of the system. For each imposed frequency of the rotating valve, the amplitude of the recorded steady oscillation is plotted. This has been done for each of the four dynamic pressure transducers. The problem is that the locations of nodes and anti-nodes shift with frequency, so that the pressures recorded at K1-K4 are not necessarily the largest pressures in the system. The picture is not fully clear, but the first resonance frequency is 4.5–5 Hz and the second is 12–13 Hz. The lowest frequency corresponds to a quarter-length mode, since the pressure amplitude increases from reservoir to outlet (K1-K2-K4-K3). Figure 13 displays results obtained on four consecutive days; the wavespeed may vary per day.

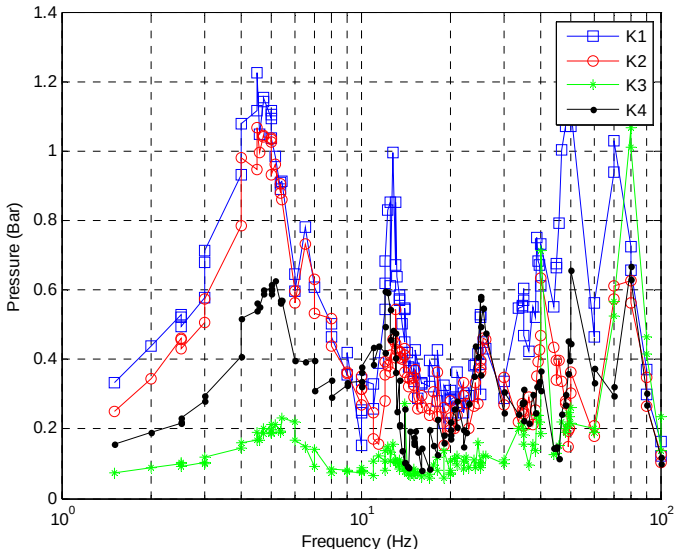

Figure 13 Measured pressure amplitudes at four locations along the pipeline versus frequency of oscillation of the rotating valve.

SIMULATIONS

Orifice model

The orifice is a horizontal slit of 100 mm width and 8 mm height. In preliminary tests and simulations [1, 2] the orifice was covered between 0% and 20% by the rotating disc (α = 1/5) in order to minimise friction (and wear) while sliding in between its guiding steel plates. The outflow area varied between 800 mm^2 and 640 mm^2. In the final tests reported herein the orifice area varied in between 240 mm^2 and 80 mm^2 (α = 2/3).

The area and resistance coefficient of the orifice in its most open position are $A_{or,0}$ = 240 mm^2 and ξ_0 = 53570 (see below). With a frictionless pipe at constant initial pressure $P_0 = P_{res}$ = 235 kPa, this gives a constant initial flow velocity V_0 = 0.0937 m/s. The neglected steady pressure loss due to skin friction along the

pipeline is $\lambda(L/D)(\rho V_0^2/2) = 21$ Pa = 0.21 mbar, assuming that $\lambda = 0.02$. This is very small compared to the steady pressure loss P_0 at the orifice. The skin friction loss is therefore negligible.

Initially the orifice is fully open. At $t = 0$ the outflow is interrupted by a frequency-controlled rotating disc that has three sinusoidal variations of 10 mm amplitude in its 263 mm radius as drawn in Fig. 4. The specific function $\tau(t)$ used to describe the orifice with rotating disc is [1, 2]:

$$\tau(t) := \frac{2}{3} + \frac{1}{3}\cos\left(2\pi\frac{t}{T}\right),$$

to be applied in $\Delta P_0\, V|V| = \tau^2(t)\, V_0|V_0| \,\Delta P$, $V_0 \neq 0$,

in which T is the period of the induced oscillation. The frequency ($f = 1/T$) range studied herein is from 1.5 Hz to 100 Hz. In its most closed position at $t/T = 1/2$ (mod 1) the orifice is a horizontal slit of 10 mm width and 8 mm height (Fig. 4) with resistance coefficient $\xi = 482132$ and flow velocity $V = 0.0312$ m/s. If $\tau(t) = 2/3$ (average τ-value) for $A_{or,av} = 160$ mm^2, then $\xi_{av} = 120533$ and $V_{av} = 0.0625$ m/s. Thus, the velocity amplitude for slow (quasi-steady, $f < 1$ Hz) variations is $\hat{V} = 0.00312$ m/s. The corresponding acoustic pressure variation (Joukowsky) is $\rho c\hat{V} = 3.94$ kPa = 39.4 mbar.

Input data

The following input data are used in the numerical simulations (using conventional nomenclature [1, 2]): $L = 49$ m, $D = 206$ mm, $e = 5.9$ mm, $H_{res} = 24$ m, $P_{atm} = 101.3$ kPa, $\rho = 999$ kg/m^3, $\lambda = 0$ (skin friction ignored herein), $\nu = 10^{-6}$ m^2/s, $g = 9.807$ m/s^2, $K = 2.17$ GPa, $E = 210$ GPa and $C_{or} = 0.6$. This input yields the derived data: $A = 33329$ mm^2, $A_{or,0} = 240$ mm^2, $\xi_0 = 53570$, $P_0 = 235$ kPa, $V_0 = 0.0937$ m/s, $Q_0 = 3.12$ L/s, $\mathrm{Re}_0 = 19310$, $c = 1025$ m/s, $c/(4L) = 5.2$ Hz and $c/(2L) = 10.5$ Hz. The material properties of water (at atmospheric pressure and 19° Celsius temperature) and steel are taken from handbooks. The length of the pipeline is rounded to 49 m, because it is not exactly clear where acoustic waves reflect at the upstream boundary. This reflection point may depend on the frequency of the steady oscillatory oscillation. The influence of the 1000 mm diameter supply pipe (instead of a constant-head reservoir) is not entirely negligible because it makes the fundamental frequency drop by 4% as shown in [2]. The greatest uncertainty is in the sonic speed c. This is quite common in the measurement of waterhammer events [8]. For example, c is very sensitive to small amounts of air in the water. One possibility is to tune the numerical results to the experimental results for one fixed frequency, say 10 Hz, and do all other calculations with the so found wavespeed. However, herein we take an average wavespeed of 1025 m/s as estimated (above) from the measurements by the methods *i)* and *iii)*.

Theory

Because $\gamma = \xi_0 V_0/c = 4.9 > 1$, the orifice is seen as a closed end by pressure waves travelling in the pipeline; see the Appendix in [2]. This means that the fundamental frequency of free vibration is $c/(4L) = 5.2$ Hz with the second mode at 15.7 Hz. The measured values in Fig. 13 are 4.5–5 Hz and 12–13 Hz. The "double-pipe" correction presented in [2] brings down the theoretical fundamental frequency to 5.0 Hz. The compliant PIV box made of Perspex and located 7.6 m upstream of the orifice may have some influence too; it may act as a storage (capacitance) element [9].

Numerical results

Exact time-domain simulations based on the method of characteristics [10, 11] have been carried out to accommodate the nonlinear orifice condition. Preliminary results for 10 Hz excitation are shown in Fig. 14. Comparing Figs 11b and 14b, it is seen that the average flow rate in the numerical simulation is far too low. The authors attribute this to leakage at the outlet. Some clearance was allowed here – at the expense of leakage – to have a smoothly running disc. If one accommodates this inevitable leakage by taking a larger discharge coefficient $C_{or} = 1$, one obtains the numerical results shown in Fig. 15. (The value of C_{or} is an uncertainty anyhow: it depends on time because of the changing aperture and it depends on frequency because of unsteadiness.) Comparing Figs 10b and 15a, one sees that the pressure amplitudes in numerical simulation and physical experiment are roughly the same. The same holds for the 12.5 Hz results, but not so for the 5 Hz results, where the predicted pressure amplitudes are up to a factor three too large.

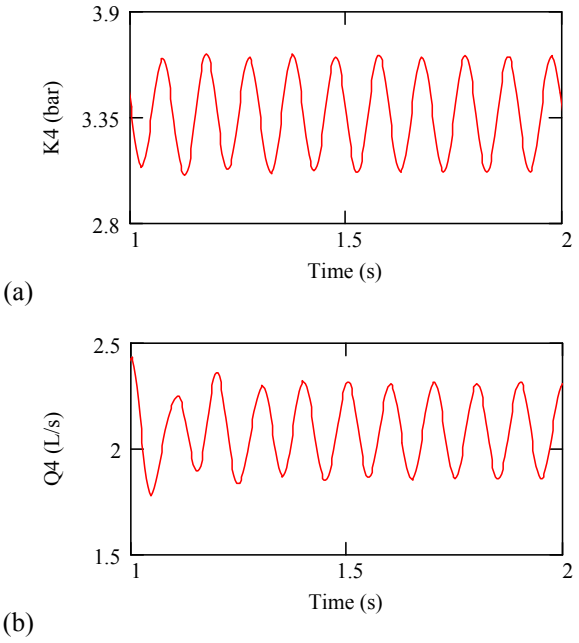

Figure 14 Numerical results for 10 Hz frequency of excitation and $C_{or} = 0.6$: (a) pressure (absolute) at position K4, (b) flow rate at position Q4.

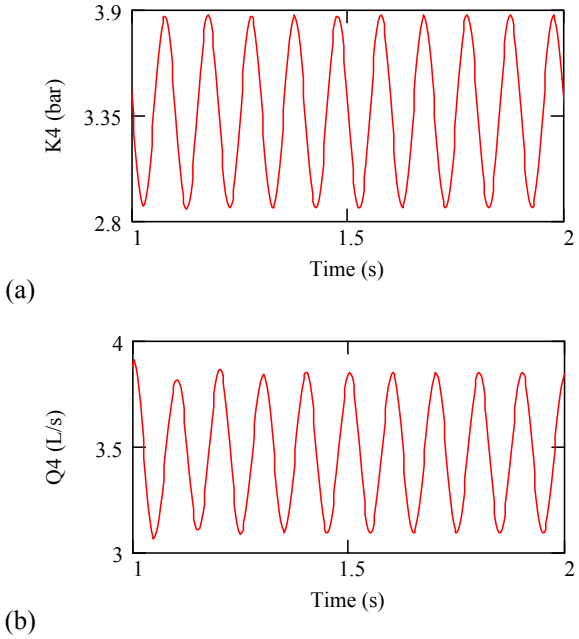

Figure 15 Numerical results for 10 Hz frequency of excitation and $C_{or} = 1$: (a) pressure (absolute) at position K4, (b) flow rate at position Q4.

CONCLUSIONS

Acoustic resonance experiments carried out in a steel pipeline filled with water have been fully described and some distinctive results have been presented. The system was excited with a specially designed rotating valve. Experimental uncertainties and sensitivities, of which the speed of sound and the orifice resistance are the most important ones, have been discussed. The results of preliminary numerical simulations do not (yet) fully match the measured data. Excessive pipe vibration was observed and recorded at resonance.

ACKNOWLEDGEMENTS

This study is part of the project *Unsteady friction in pipes and ducts* carried out at Deltares, Delft, The Netherlands, and was partially funded through EC-HYDRALAB III Contract 022441 (R113) by the European Union. The Chinese Ministry of Education is thanked for financially supporting the second author. Hugo Hartmann (Deltares), Sandy Anderson (Newcastle University), Sašo Vučkovič (Litostroj) and Rok Mavrič (University of Ljubljana) assisted in the laboratory measurements and data analysis.

REFERENCES

[1] Tijsseling A.S., Hou Q., Svingen B. and Bergant A. (2010) Acoustic resonance in a reservoir-pipeline-orifice system. Proceedings of the 2010 ASME Pressure Vessels and Piping Division Conference, Bellevue, Washington, USA, Paper PVP2010-25083.

[2] Tijsseling A.S., Hou Q., Svingen B. and Bergant A. (2012) Acoustic resonance in a reservoir – double pipe – orifice system. Proceedings of the 2012 ASME Pressure Vessels and Piping Division Conference, Toronto, Canada, Paper PVP2012-78085.

[3] Vardy A.E., Bergant A., He S., Ariyaratne C., Koppel T., Annus I., Tijsseling A.S. and Hou Q. (2009) Unsteady skin friction experimentation in a large diameter pipe. Proceedings of the 3rd IAHR International Meeting of the Workgroup on Cavitation and Dynamic Problems in Hydraulic Machinery and Systems (Editor P. Rudolf), Brno, Czech Republic, pp. 593-602.

[4] Ariyaratne C., He S. and Vardy A.E. (2010) Wall friction and turbulence dynamics in decelerating pipe flows. IAHR Journal of Hydraulic Research 48, 810-821.

[5] Annus I. and Koppel T. (2011) Transition to turbulence in accelerating pipe flow. ASME Journal of Fluids Engineering 133 / 071202, 1-9.

[6] He S., Ariyaratne C. and Vardy A.E. (2011) Wall shear stress in accelerating turbulent pipe flow. Journal of Fluid Mechanics 685, 440-460.

[7] Svingen B. (1996) Fluid-structure interaction in slender pipes. BHR Group, Proceedings of the 7th International Conference on Pressure Surges and Fluid Transients in Pipelines and Open Channels (Editor A. Boldy), Harrogate, U.K., pp. 385-396.

[8] Thorley A.R.D. (1971) Influence of variations of transient velocity on resonating frequencies. Proceedings of the Symposium on State-of-the-Art of Fluid Transients, ASME Winter Annual Meeting, Washington D.C., USA, Paper 71-WA/FE-20.

[9] Wylie E.B., Streeter V.L. and Suo L. (1993) *Fluid Transients in Systems*, Englewood Cliffs: Prentice Hall, Section 13-8.

[10] Tijsseling A.S. and Bergant A. (2007) Meshless computation of water hammer. Proceedings of the 2nd IAHR International Meeting of the Workgroup on Cavitation and Dynamic Problems in Hydraulic Machinery and Systems (Editors R. Susan-Resiga, S. Bernad and S. Muntean), Timişoara, Romania, Scientific Bulletin of the "Politehnica" University of Timişoara, Transactions on Mechanics, Vol. 52(66), No. 6, pp. 65-76, ISSN 1224-6077.

[11] Tijsseling A.S. and Bergant A. (2012) Exact computation of waterhammer in a three-reservoir system. BHR Group, Proceedings of the 11th International Conference on Pressure Surges (Editor Sandy Anderson), Lisbon, Portugal, pp. 161-170, ISBN 978-1-85598-133-1.